

# High Capacity Sulfur-Porous Carbon Composite for Positive Electrode of Lithium Batteries

Heisuke Nishikawa\*    Shuji Hitomi\*    Hiroaki Yoshida\*

## Abstract

High capacity sulfur-porous carbon composite has been synthesized by using MgO templated carbon matrix having nano-sized uniform pore. This composite showed extremely high discharge capacity of  $1080 \text{ mAh g}^{-1}$  based on the mass of the composite. This is derived from the fact that high content sulfur of 70 mass% in the composite exists in the fine pore resulting in high utilization of sulfur for electrochemical reaction. It was found that the utilization of sulfur in the composite positive electrode by using polyethylene imine (PEI) as a binder is higher than the case of Poly(vinylidene fluoride) (PVdF). This improvement is due to the fact that the charge transfer resistance of the former electrode is lower than that of the latter electrode due to a good electric conductive network formation judging from electrochemical impedance spectroscopy (EIS). This is caused by the uniform dispersibility of the electrode materials in the PEI type electrode.

*Key words*: Lithium; Sulfur; MgO templated carbon; Polyethylene imine

## 1 Introduction

Sulfur has been recognized as one of the most promising candidate of the positive active material for the next-generation high energy density lithium secondary battery because it has high theoretical capacity of  $1675 \text{ mAh g}^{-1}$  and is additionally low cost, an abundant resource, and being environmentally friendly. However, due to the insulating nature of sulfur and  $\text{Li}_2\text{S}$  of its discharge product, a large amount of conductive agent must be employed in the electrode, which offsets the high theoretical capacity. Recently, extensive researches for composite technologies of sulfur and carbon matrices such as carbon nano tube, graphene, and mesoporous carbon have been carried out to solve this problem.<sup>1-5</sup> However, the discharge capacity based on the mass of the composite still re-

mains below  $800 \text{ mAh g}^{-1}$  because these matrices have large sized pores, inhomogeneous pore distribution and inadequate pore volume for high sulfur loading amount, resulting in extremely poor dispersibility of sulfur with low utilization. In this study, the sulfur-porous carbon composite with large amount and high utilization of sulfur was synthesized by using MgO templated porous carbon as a carbon matrix having nano-sized homogeneous pore and high pore volume. Furthermore, it is demonstrated that the applying PEI as an aqueous binder instead of a conventional PVdF binder improves the electrochemical performance of the sulfur composite electrode.

## 2 Experimental

### 2.1 Preparation

The porous carbon was synthesized by MgO template derived from magnesium citrate.<sup>6</sup> The magne-

\* Department II, R & D Center

sium citrate was used as the precursor of the carbon and also provided the nano-sized MgO particles template. The magnesium citrate was heated to 900°C under N<sub>2</sub> atmosphere with a heating rate of 5°C min<sup>-1</sup>, and maintained at this temperature for 1 h. Obtained carbon-MgO composite was treated by 1M H<sub>2</sub>SO<sub>4</sub> for removing MgO. Subsequently, this composite was washed by H<sub>2</sub>O and dried at 100°C for 12 h.

The sulfur-porous carbon composite was prepared as follows. The porous carbon was mixed with sulfur powder in a mass ratio of 3 : 7. And then, this mixture was heated at 150°C for 5 h followed by 300°C for 2 h in a sealed vessel filled with Ar. Sulfur-Ketjenblack (600JD) composite for comparison was synthesized in the same way.

## 2.2 Characterization

The sulfur content of the composites was checked by the thermogravimetric analysis (TGA, PerkinElmer) at a heating rate of 10°C min<sup>-1</sup> from room temperature to 500°C in He atmosphere. A nitrogen adsorption isotherm was measured by an automated gas sorption system (Autosorb, Quantachrome). The surface area and pore size distribution of the carbon matrix and the sulfur composite were calculated using the Brunauer-Emmett-Teller (BET) theory and the Barrett-Joyner-Halenda (BJH) for a mesopore region and the non-linear density function theory (NLDFT) method for a micropore region. The total pore volume was obtained at a relative pressure of 0.99. The microstructure and morphology of all samples were examined using a scanning and transmission electron microscopy (STEM, Hitachi). The electric conductivities of the carbon matrices and composites were calculated by powder resistivity measurement (Mitsubishi chemical analytech).

## 2.3 Electrochemical property

The positive electrode slurry was prepared by mixing 85 mass% sulfur-carbon composite, 5 mass% acetylene black as a conductive agent, and 10 mass% PVdF binder in NMP (N-methyl-2-pyrrolidone). In the case of PEI as a binder, the slurry was prepared by using water as a solvent instead of NMP. These slurry were pasted on a Ni substrate and dried at 100°C for 12 h. The positive electrodes were incorporated into two electrode type test cells in a glove box filled

with Ar, using lithium metal as the negative electrode, a polyethylene microporous membrane as a separator and 1M bis-(trifluoromethane sulfonyl) imide in a solvent of tetraethylene glycol dimehty ether (TEGDME) as a electrolyte solution. The galvanostatic discharge tests were carried out at a constant current of 0.1 C (167.5 mA g<sup>-1</sup>-sulfur, average sulfur loading in the electrode 1 mg cm<sup>-2</sup>) in the voltage range of 1.0 to 3.0 V. The electrochemical impedance spectroscopy (EIS) measurements of these test cells were carried out at open-circuit potential in the frequency range between 100 kHz and 10 mHz with perturbation amplitude of 5 mV.

## 3 Results and discussion

### 3.1 Structural analysis of sulfur-carbon composites

Morphologies of MgO templated porous carbon and Ketjenblack observed by SEM and TEM are shown in Fig. 1 and 2, respectively. The porous carbon is found

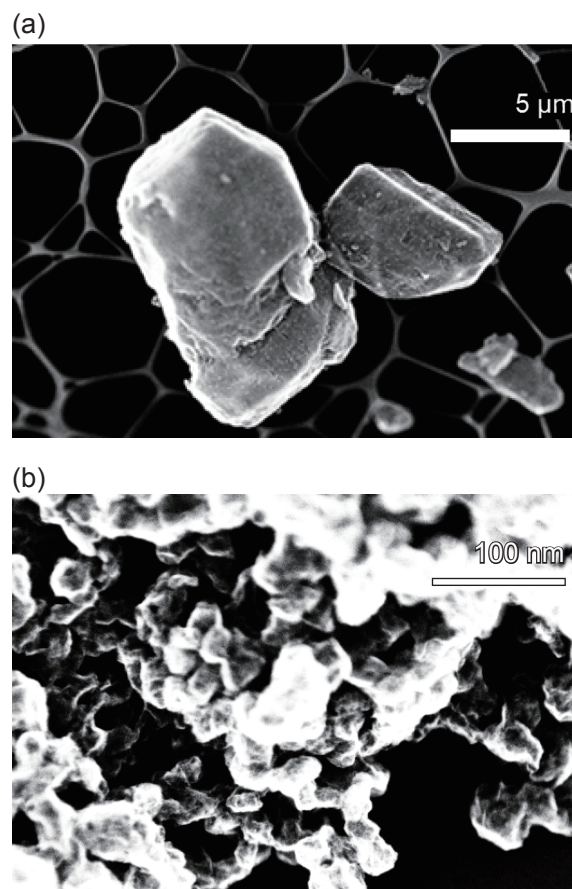


Fig. 1 SEM images for porous carbon (a) and Ketjenblack (b) on Cu microgrid for STEM.

out to have primary particles with more than  $5 \mu\text{m}$  of diameter, in which extremely fine pores exist. On the other hand, Ketjenblack is in condensed state with primary particles with about 30 nm of diameter having hollow structure. Pore size distributions of both carbon matrices are shown in Fig. 3. It is found out that uniform primary pores with 3 nm at peak top distribute in the porous carbon, whereas Ketjenblack has primary pores with the same size as that of porous carbon arising from the hollow structure and larger size secondary pores of more than 10 nm. BET surface areas and total pore volumes of porous carbon and Ketjenblack are shown in Table 1. The sulfur content in the obtained sulfur-carbon composites are confirmed by TGA. As shown in Fig. 4, both composites have 70 mass% sulfur calculated by weight loss during room temperature to  $500^\circ\text{C}$ . Changes in pore distribution and cumulative pore volume before and

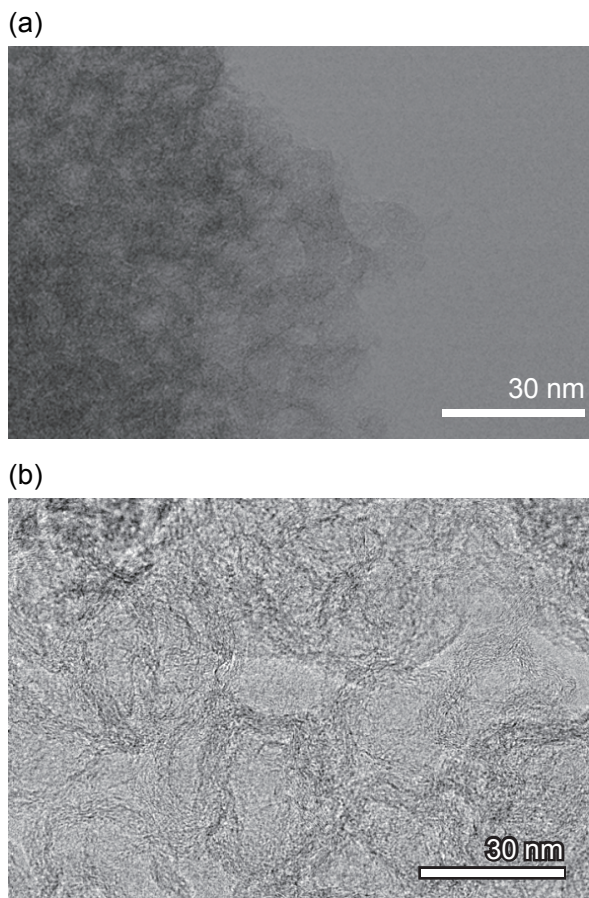


Fig. 2 TEM images for porous carbon (a) and Ketjenblack (b).

after sulfur loading are shown in Fig. 5. Pores almost disappeared after the loading, although both carbon matrices have adequate total pore volume (Table 1) for encapsulating the sulfur with  $1.1 \text{ cm}^3 \text{ g}^{-1}$  of occupancy volume corresponding to 70 mass% -sulfur. Electric conductivities of carbon matrices and the sulfur-carbon composites are plotted as a function of pressing pressure for the sample in Fig. 6. The con-

Table 1 Surface area and pore volume of porous carbon and Ketjenblack.

Materials	Porous carbon	Ketjenblack
Surface area / $\text{cm}^2 \text{ g}^{-1}$	2400	1023
Pore volume / $\text{cm}^3 \text{ g}^{-1}$	2.1	1.7

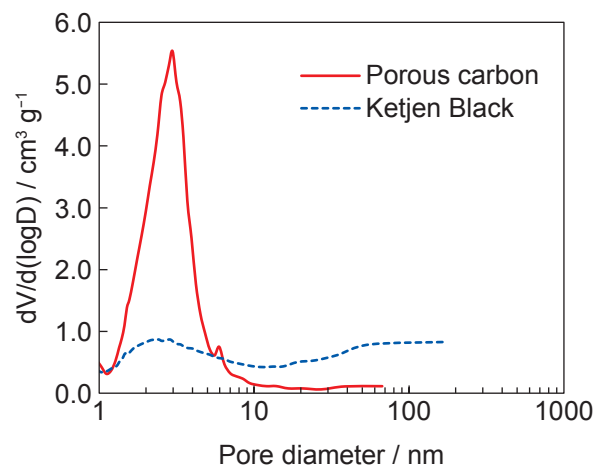


Fig. 3 Pore distributions for porous carbon and Ketjenblack.

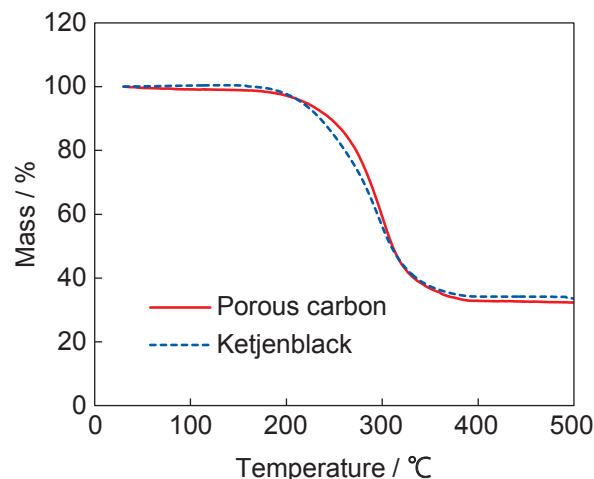


Fig. 4 Tg curves for sulfur-carbon composites.

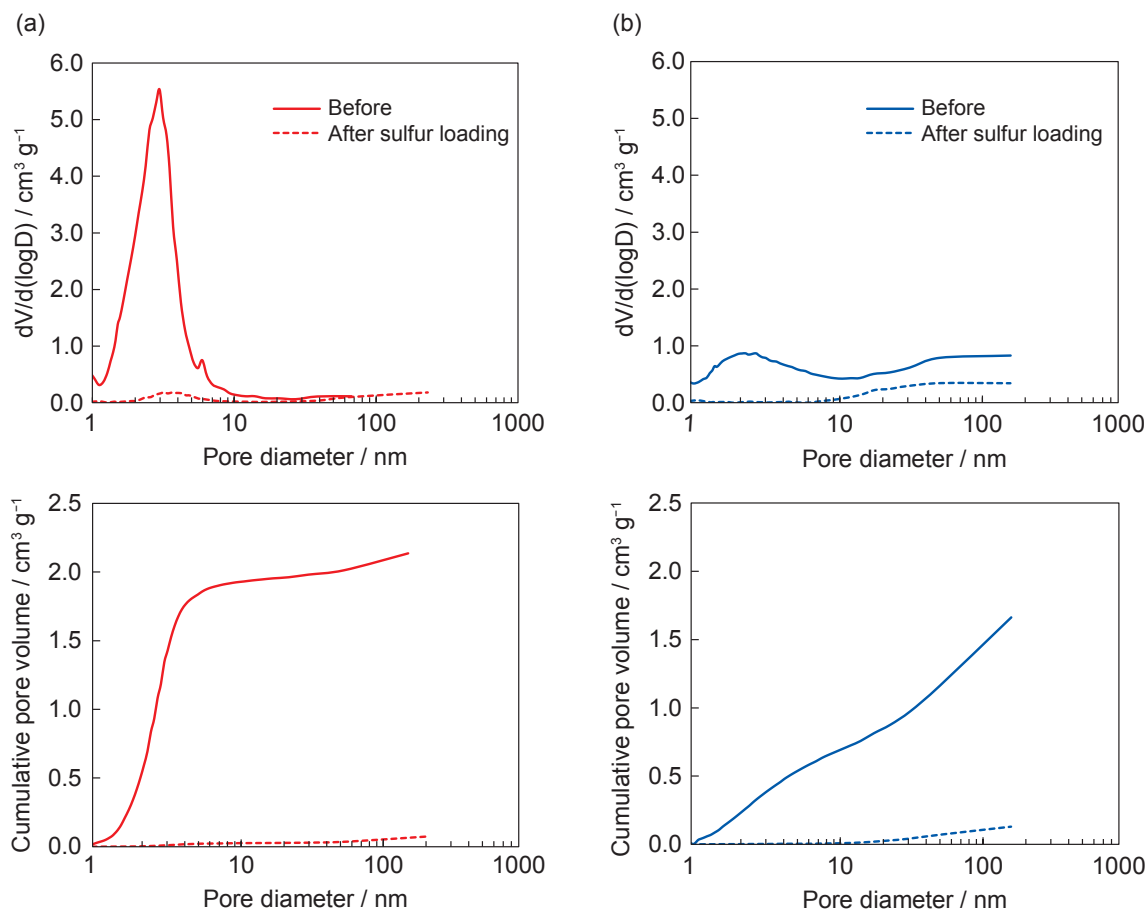


Fig. 5 Pore distributions and cumulative pore volume for porous carbon (a) and Ketjenblack (b) before and after sulfur loading.

ductivity of the composite of Ketjenblack noticeably decreases after sulfur loading. On the other hand, in the case of the porous carbon composite, the conductivity does not change before and after the loading. These results are derived from the difference of insulating sulfur loading states and suggest that porous carbon having large pore volume of primary pore with size of 3 nm is able to contain sulfur of 70 mass% into the pore, meanwhile Ketjenblack has only  $0.7 \text{ cm}^3 \text{ g}^{-1}$  primary pore volume which is insufficient for the total mass of sulfur and then the part of sulfur with large particle size exists at secondary pores, in other words, the carbon surface, resulting in decrease of conductivity of the composite.

### 3.2 Electrochemical performance of sulfur-carbon composites

Discharge performance of the sulfur-porous carbon composite positive electrode with PVdF binder compared to that of Ketjenblack is shown in Fig. 7. The

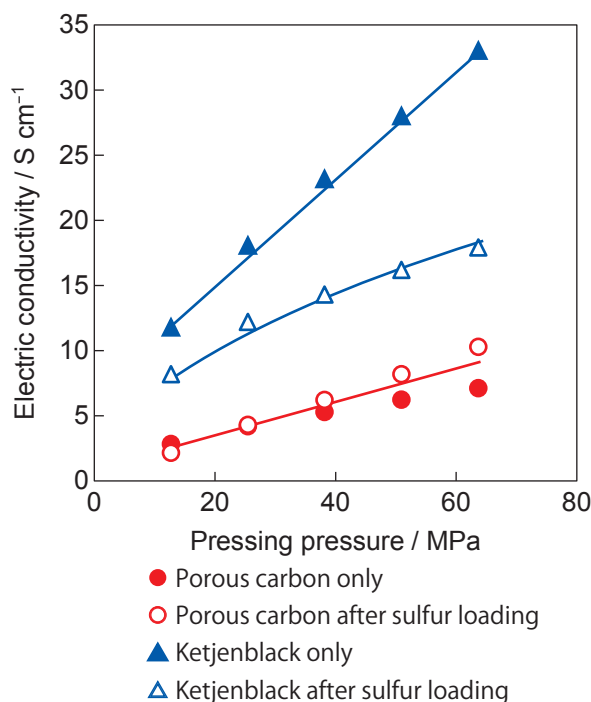


Fig. 6 Electric conductivity for porous carbon and Ketjenblack before and after sulfur loading.

sulfur-porous carbon composite shows higher discharge capacity ( $855 \text{ mAh g}^{-1}$ , based on mass of the composite) than that of Ketjenblack ( $574 \text{ mAh g}^{-1}$ ). The sulfur utilizations of porous carbon and Ketjenblack composites calculated from the value of percentage of discharge capacity to theoretical capacity divided by the sulfur contents are 73 and 49%, respectively. This difference of the utilizations is derived from the fact that high amount sulfur of 70 mass% with fine particle size is able to be uniformly distributed in the porous carbon composite, resulting in high contributing ratio for electrochemical reaction, whereas sulfur with large particle size existing on the surface of Ketjenblack does not contribute the reaction. Furthermore, it was found out that this sulfur utilization is increased by selecting the suitable electrode binder. As shown in Fig. 8 of discharge performances, the sulfur-porous carbon composite positive electrode by using a new aqueous binder of PEI shows higher discharge capacity than that of the electrode by using a conventional PVdF binder. The PEI type electrode has achieved discharge capacity of  $1080 \text{ mAh g}^{-1}$  (based on mass of the composite). This value means the high sulfur utilization of 93%. Fig. 9 represents the EIS analysis of Li/S cells with PEI and PVdF type electrodes at open circuit voltage after assembling the cells. In these Cole-Cole plots, the semi-circles correspond to the total of charge-trans-

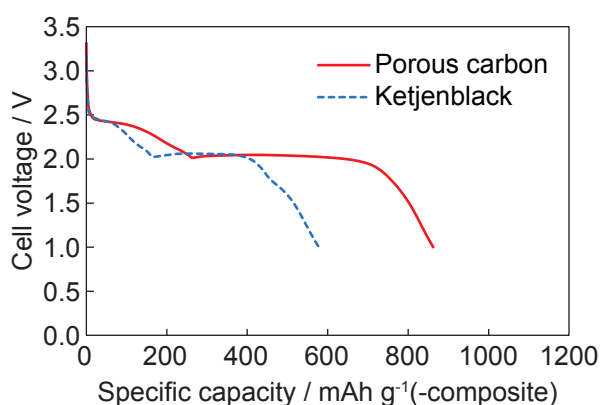


Fig. 7 Discharge performances for the Li/S cells with sulfur-carbon composites at  $25^\circ\text{C}$  using  $1 \text{ M LiTFSI}$  in TEGDME (Composite : AB : PVdF = 85 : 5 : 10). The discharge current and cutoff voltage ;  $0.1 \text{ C}$  ( $167.5 \text{ mA g}^{-1}$ -sulfur) and  $1.0 \text{ V}$ .

fer resistances at negative and positive electrodes and bulk resistance of SEI on a lithium surface. The resistances of the negative electrode are same between PEI and PVdF electrodes. Therefore, difference of the resistances means difference of charge-transfer resistance at positive electrodes. The resistance of the PEI type electrode is found out to be lower than that of the PVdF type one. To investigate this difference of the resistance, the surface of the PEI and PVdF electrodes were observed by SEM. Fig. 10 shows the sur-

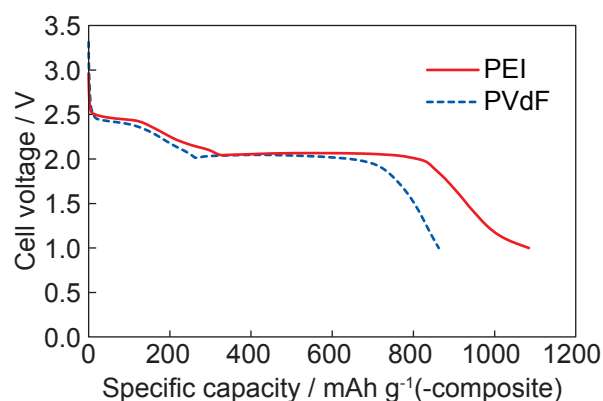


Fig. 8 Discharge performances for the Li/S cells with sulfur-porous carbon composite electrodes by using different types of binders at  $25^\circ\text{C}$  using  $1 \text{ M LiTFSI}$  in TEGDME (Composite : AB : Binder = 85 : 5 : 10 mass%). The discharge current and cutoff voltage ;  $0.1 \text{ C}$  ( $167.5 \text{ mA g}^{-1}$ -sulfur) and  $1.0 \text{ V}$ .

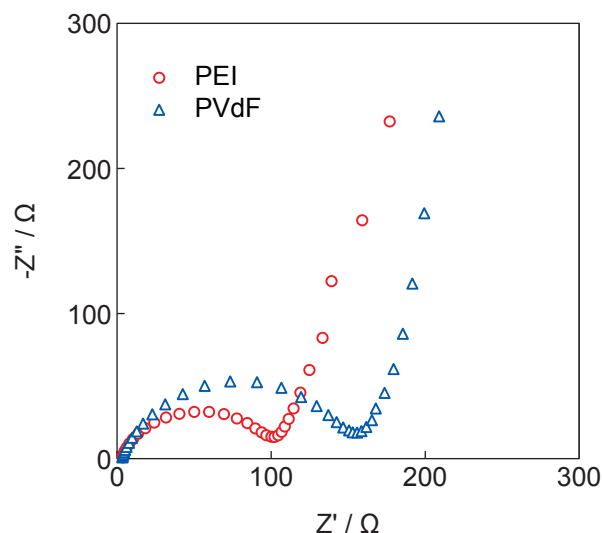
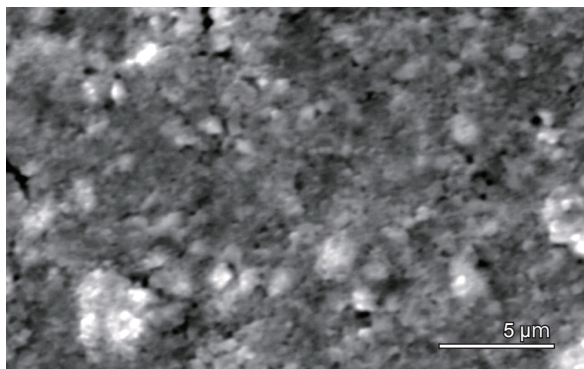


Fig. 9 Cole-Cole plots for the Li/S cells with sulfur-porous carbon composite electrodes by using different types of binders at  $25^\circ\text{C}$  using  $1 \text{ M LiTFSI}$  in TEGDME.

(a) PEI



(b) PVdF

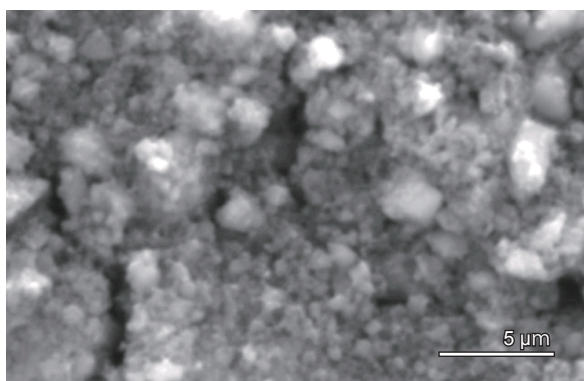


Fig. 10 SEM images for the sulfur-porous carbon composite electrodes with different types of binders; (a) PEI and (b) PVdF.

face morphologies of both electrodes. The surface morphology of the PEI type electrode is smooth and electrode materials are uniformly distributed, while in the PVdF type electrode, there are aggregation of the electrode materials and some cracks. It is considered that this aggregation in the PVdF type electrode brings an insufficient electric conductive network. These results support the difference of charge-transfer resistances. It is concluded that sulfur utilization in the PEI type electrode increases to higher value compared to that of the PVdF one because of the good electric conductive network in the electrode.

## 4 Conclusion

Lithium/sulfur battery with a sulfur-MgO templated porous carbon composite positive electrode containing a PEI binder successfully achieved to show high discharge capacity, more than  $1000 \text{ mAh g}^{-1}$  based on the mass of the composite. This high capacity is derived from the fact that sulfur with high content of 70 mass% exist in the pore with fine particle size because the porous carbon has high pore volume and nano-sized uniform pore, resulting in high sulfur utilization. Furthermore, it was clarified that the charge-transfer resistance of the sulfur-porous carbon composite positive electrode by applying a PEI binder effectively decreased compared to that of a PVdF type electrode due to the good electric conductive network in the electrode.

## References

1. Juchen Guo, Yunhua Xu, and Chunsheng Wang, *Nano Letters*, **11**, 4288 (2011).
2. Yuliang Cao, Xiaolin Li, Ilhan A. Aksay, John Lemmon, Zimin Nie, Zhenguo Yang, and Jun Liu, *Phys. Chem. Chem. Phys.*, **13**, 7660 (2011).
3. Liwen Ji, Mumin Rao, Haimei Zhang, Yuanchang Li, Wenhui Duan, Jinghua Guo, Elton J. Cairns, and Yuegang Zhang, *Journal of The American Chemical Society*, **133**, 18522 (2011).
4. Xiaolim Li, Yuliang Cao, Wen Qi, Laxmikant V. Saraf, Jie Xiao, Zimin Nie, Jaromir Mietek, Ji-Guang Zhang, Birgit Schwenzer, and Jun Liu, *Journal of Materials Chemistry*, **21**, 16603 (2011).
5. Jorg Schuster, Guang he, Benjamin Mandlmeier, Taeun Yim, Kyu Tae Lee, Thomas Bein, and Linda F. Nazar, *Angewandte Chemie Int. Ed.* **51**, 3591 (2012).
6. Hironori Orikasa and Takahiro Morishita, *TANSO*, **254**, 153 (2012).